

See discussions, stats, and author profiles for this publication at: <https://www.researchgate.net/publication/11212431>

High Resolution 3D Exchange NMR Spectroscopy and the Mapping of Connectivities between Half-integer Quadrupolar Nuclei

ARTICLE *in* JOURNAL OF THE AMERICAN CHEMICAL SOCIETY · SEPTEMBER 2002

Impact Factor: 12.11 · DOI: 10.1021/ja020534v · Source: PubMed

CITATIONS

29

READS

16

3 AUTHORS, INCLUDING:



Mattias Edén

Stockholm University

109 PUBLICATIONS 2,980 CITATIONS

SEE PROFILE



Lucio Frydman

Weizmann Institute of Science

220 PUBLICATIONS 6,126 CITATIONS

SEE PROFILE

High Resolution 3D Exchange NMR Spectroscopy and the Mapping of Connectivities between Half-integer Quadrupolar Nuclei

Mattias Edén,[†] Julia Grinshtein, and Lucio Frydman*

Department of Chemical Physics, Weizmann Institute of Sciences, 76100 Rehovot, Israel

Received April 15, 2002; Revised Manuscript Received June 8, 2002

The nuclear magnetic resonance (NMR) of spin $S > 1/2$ nuclei is usually dominated by their quadrupolar nature.¹ Due to the anisotropy of this interaction, solid-state spectra of half-integer quadrupole nuclei have generally been restricted to the observation of central $-1/2 \leftrightarrow +1/2$ transitions. Central single-quantum transitions, however, are not generally sharp; they are affected by second-order quadrupole effects which, even though smaller than their first-order counterparts, can still broaden resonances from chemically inequivalent sites by several kHz.¹ During the past few years a number of techniques such as multiple-quantum magic-angle-spinning (MQMAS), have been proposed for the acquisition of high-resolution spectra where NMR resonances appear devoid of all quadrupolar anisotropies.² As the use of these quadrupolar NMR techniques expands, voids in the current understanding of how to assign the peaks that these methods can resolve become increasingly evident. Among the few unambiguous approaches available for the assignment of solid-state quadrupole resonances are those relying on the spin–spin coupling between the nuclei under observation and their NMR-active neighbors.³ A number of MQMAS variants have been described and demonstrated where dipolar couplings in heteronuclear systems involving quadrupoles are monitored.⁴ In the present communication we describe an extension of these measurements to an isotropic 3D NMR version applicable to *homonuclear* systems, and the results observed upon applying such high-resolution experiments on a model three-site ²³Na salt.

Monitoring spin–spin couplings between nonbonded homonuclei commonly relies on exchange-type NMR sequences.⁵ When dealing with anisotropic line shapes these experiments can reveal, via off-diagonal cross-peaks, dynamics and relative orientations between related nuclei. Yet such anisotropic measurements are restricted to a limited number of inequivalent chemical sites whose patterns do not overlap; if this is not the case, resolution can still be achieved by introducing a third spectral dimension capable of encoding a purely isotropic evolution.⁶ Different strategies can be adopted when extending such procedures to multisite spin systems affected by second-order quadrupolar anisotropies. One such possibility is illustrated in Figure 1. This pulse sequence resembles a basic split- t_1 z-filtered MQMAS experiment,⁷ with the introduction of a redefined evolution period following the multiple- to single-quantum conversion step. From the conventions illustrated in the Figure it follows that spins will first undergo a purely isotropic evolution ν_{iso} during the time t_1 , an initial anisotropic encoding $\nu_{\text{aniso}}^{(i)}$ during t_2 , and a final anisotropic precession $\nu_{\text{aniso}}^{(f)}$ during the acquisition time t_3 . The overall time-domain signal will then be given by

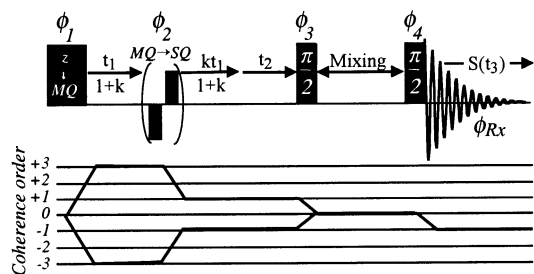


Figure 1. Pulse sequence proposed for the acquisition of isotropically resolved exchange correlation spectra on half-integer quadrupoles. In the actual implementation of the experiment the following phase cycling scheme was used (in degrees): $\phi_1 = \{0, 60, 120, 180, 240, 300\}$; $\phi_2 = \{0, 90, 180, 270\}$; $\phi_4 = \{0, 90, 180, 270\}$. ϕ_3 was set to $\{0\}$ and $\{90\}$ to record cosine- and sine-modulated data respectively; ϕ_{Rx} was cycled to retrieve the illustrated coherence transfer pathway.

$$S_{\cos}(t_1, t_2, t_3) = \iiint I(\nu_{\text{iso}}, \nu_{\text{aniso}}^{(i)}, \nu_{\text{aniso}}^{(f)}) \cos$$
$$[\nu_{\text{iso}} t_1 + \nu_{\text{aniso}}^{(i)} t_2] \exp(i\nu_{\text{aniso}}^{(f)} t_3) d\nu_{\text{iso}} d\nu_{\text{aniso}}^{(i)} d\nu_{\text{aniso}}^{(f)} \quad (1)$$
$$S_{\sin}(t_1, t_2, t_3) = \iiint I(\nu_{\text{iso}}, \nu_{\text{aniso}}^{(i)}, \nu_{\text{aniso}}^{(f)}) \sin$$
$$[\nu_{\text{iso}} t_1 + \nu_{\text{aniso}}^{(i)} t_2] \exp(i\nu_{\text{aniso}}^{(f)} t_3) d\nu_{\text{iso}} d\nu_{\text{aniso}}^{(i)} d\nu_{\text{aniso}}^{(f)}$$

Fourier analysis reveals that the cosine-modulated signal will lead to in-phase purely absorptive correlation peaks at coordinates $[\pm(\nu_{\text{iso}}, \nu_{\text{aniso}}^{(i)}, \nu_{\text{aniso}}^{(f)})]$, whereas S_{\sin} will yield anti-phase doublets at the same set of frequencies; 3D hypercomplex processing then results in purely absorptive $I(\nu_{\text{iso}}, \nu_{\text{aniso}}^{(i)}, \nu_{\text{aniso}}^{(f)})$ spectra, with quadrature detection along all three frequency axes.

This 3D MQMAS/exchange strategy was explored on Na_2SO_3 using the NMR of ²³Na, a 100% abundant spin- $3/2$ nucleus, as a model. This salt possesses three crystallographically inequivalent sites,^{8a} whose MAS powder line shapes overlap at the 4.7-T field employed in the present study but are resolved by MQMAS.^{8b,c} Conventional 2D exchange MAS NMR experiments exhibit extensive off-diagonal cross-peaks for this compound (Figure 2A). These exchange powder line shapes occur despite the absence of protons in this lattice and stem in part from the MAS-driven dipolar recoupling induced by modulation of the first-order quadrupolar interaction.⁹ Figure 3 illustrates the results afforded by the 3D MQMAS NMR experiment when applied on powdered Na_2SO_3 , showing an isotropic projection and the single-quantum/single-quantum 2D correlation spectra extracted orthogonal to the isotropic frequencies of individual sites. An unusual distinction between the exchange line shapes resolved by this 3D NMR experiment vis-à-vis off-diagonal features in conventional 2D exchange MAS spectra, is the asymmetric disposition of the former about the main diagonal. This originates from the fact that high-resolution 3D sequences such as the one in Figure 1 will associate the isotropic evolution to solely

* To whom correspondence should be addressed. Fax: +972-8-9344123. E-mail: lucio.frydman@weizmann.ac.il.

[†] Present Address: Physical Chemistry Division, Arrhenius Laboratory, Stockholm University, S-106 91 Stockholm, Sweden.

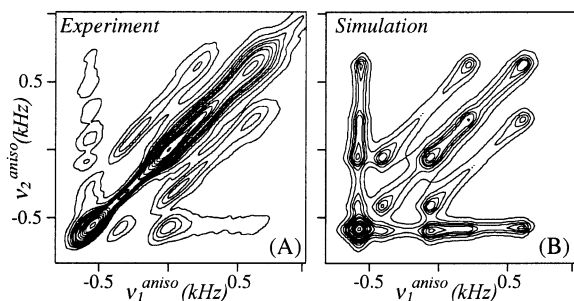


Figure 2. (A) ^{23}Na 2D exchange NMR spectrum of polycrystalline Na_2SO_3 , recorded at a spinning rate of 4100 Hz using a mixing time of 500 ms. This spectrum was obtained from rotor-synchronous echo and anti-echo data sets collected on a laboratory-built NMR spectrometer and probe operating at a 53.16 MHz Larmor frequency, with 16 scans/ t_1 , 96 total t_1 points, and a 2-s delay between scans. (B) Combined 2D exchange line shape calculated for three mutually exchanging ^{23}Na sites, stemming from the individual site-resolved line shapes shown in Figure 3.

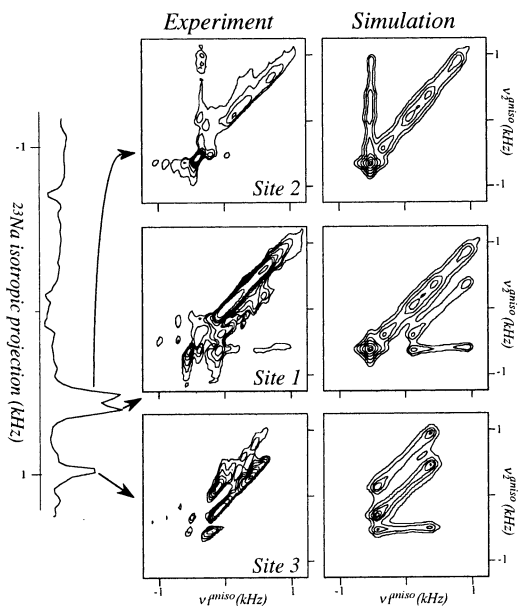


Figure 3. (Left) High-resolution 3D ^{23}Na NMR spectrum of polycrystalline Na_2SO_3 , illustrating the 2D exchange slices extracted at the indicated frequencies. Sites are labeled according to the original literature.⁸ Data were recorded using the pulse sequence in Figure 1 and conditions as in Figure 2, except for a 3800 Hz spinning rate, 40 and 28 total t_1 and t_2 points, 315- μs t_1 dwell times. 3Q excitation involved an 11- μs pulse and a 3Q \rightarrow 1Q conversion with four 6.5 μs optimized FAM pulses ($\omega_{\text{rf}}/2\pi = 40$ kHz).¹⁰ Hypercomplex data sets were combined into a single 128³ frequency spectrum upon Fourier processing. (Right) 2D exchange line shapes calculated for the corresponding sites as described in the text; the simulation of sites 1 and 2 took into account the partial isotropic overlap between these two resonances.

one of the two correlated anisotropic frequencies. Thus, the experiment separates the off-diagonal features that originate in site i and transfer into site j , from their mirror-image complements. Evidently, the overall symmetry of the off-diagonal features is restored if slices arising from all the sites involved in the exchange or spin-diffusion processes are added together.

The spin-diffusion line shapes resolved in Figure 3 facilitate the search for correlations between the identity of the peaks and their local structure. Analyzing these 2D spectral line shapes requires establishing the network of pairwise coupled proximate sites within the homonuclear system, as well as their quadrupole and isotropic shielding parameters. Quadrupole couplings and isotropic chemical shifts can be directly read from the conventional 2D MQMAS spectra, while it is clear that for the acquisition parameters employed

cross-peaks are dominated by spin-diffusion between sites 1 \leftrightarrow 3 and sites 2 \leftrightarrow 3. A full analysis of these 2D exchange line shapes reveals that because of null asymmetry parameters, the polar angle β_{13} between quadrupole tensors of sites 1 and 3 could not deviate by more than 6° from parallel. This is in very good agreement with the values estimated by Power on the basis of the compound's crystalline structure.^{8a,b} The right-hand column of Figure 3 summarizes the results arising from the various fits for the individual sites; when all these data are added up, it becomes possible to reconstruct the original single-quantum/single-quantum 2D exchange MAS NMR spectrum (Figure 2B).

The purpose of this study was to introduce a new experiment capable of extending 2D exchange NMR protocols to the analysis of homonuclear half-integer quadrupolar spin systems. This sequence bears evident resemblance to other 2D schemes emerging in the solid NMR literature,¹¹ its main difference being the implementation as a full, isotropically resolved 3D NMR acquisition. Key to the upscaling of the sequence into a third dimension was the limited use of multiple rf manipulations, a fact that made its signal-to-noise comparable to that of conventional MQMAS acquisitions. An application involving dipole-driven spin diffusion was stressed in this study; yet it is evident that interesting dynamic applications could also result. Also important to address is the nature of the various and often competing processes that can generate cross-peaks when exchange-type sequences are implemented on quadrupolar systems, a topic that will be discussed elsewhere at greater length.^{9b}

Acknowledgment. This work was supported by the U.S. Department of Energy (Grant 00ER15049), by a Philip M. Klutznick Fund for Research (Weizmann Institute), as well as by the Israeli Science Foundation (Grant 296/01). M.E. acknowledges a post-doctoral fellowship from The Swedish Foundation for International Cooperation in Research and Higher Education (STINT).

References

- (1) (a) Abragam, A. *Principles of Nuclear Magnetism*; Oxford University Press: New York, 1961. (b) Cohen, M. H.; Reif, F. *Solid State Phys.* **1957**, *5*, 321.
- (2) (a) Mueller, K. T.; Sun, B. Q.; Chingas, G. C.; Zwaniger, J. W.; Terao, T.; Pines, A. *J. Magn. Reson.* **1990**, *86*, 470. (b) Chmelka, B. F.; Zwaniger, J. W. *NMR: Basic Princ. Prog.* **1994**, *33*, 79. (c) Frydman, L.; Harwood, J. S. *J. Am. Chem. Soc.* **1995**, *117*, 5367. (d) Gan, Z. H. *J. Am. Chem. Soc.* **2000**, *122*, 3242.
- (3) (a) Bennett, A. E.; Griffin, R. G.; Vega, S. *NMR: Basic Princ. Prog.* **1994**, *30*, 3. (b) Dusold, S.; Sebald, A. *Ann. Rep. NMR Spectrosc.* **2000**, *41*, 185. (c) Frydman, L. *Annu. Rev. Phys. Chem.* **2001**, *52*, 463.
- (4) (a) Fernandez, C.; Lang, D. P.; Amoureux, J.-P.; Pruski, M. *J. Am. Chem. Soc.* **1998**, *120*, 2672. (b) Pruski, M.; Bailly, A.; Lang, D. P.; Amoureux, J.-P.; Fernandez, C. *Chem. Phys. Lett.* **1999**, *307*, 35.
- (5) (a) Jeener, J.; Meier, B. H.; Bachmann, P.; Ernst, R. R. *J. Chem. Phys.* **1979**, *71*, 4546. (b) Schmidt-Rohr, K.; Spiess, H. W. *Multidimensional Solid-State NMR and Polymers*; Academic Press: London, 1994.
- (6) (a) Frydman, L.; Lee, Y. K.; Emsley, L.; Chingas, G. C.; Pines, A. *J. Am. Chem. Soc.* **1993**, *115*, 4825. (b) Lee, Y. K.; Emsley, L.; Larsen, R. G.; Schmidt-Rohr, K.; Hong, M.; Frydman, L.; Chingas, G. C.; Pines, A. *J. Chem. Phys.* **1994**, *101*, 1852.
- (7) (a) Brown, S. P.; Heyes, S. J.; Wimperis, S. *J. Magn. Reson.* **1996**, *A119*, 280. (b) Amoureux, J. P.; Fernandez, C.; Steuernagel, S. *J. Magn. Reson.* **1996**, *A123*, 116.
- (8) (a) Larsen, L. O.; Kierkegaard, P. *Acta Chem. Scand.* **1969**, *23*, 2253. (b) Power, W. P. *Magn. Reson. Chem.* **1994**, *33*, 220. (c) Medek, A.; Harwood, J. S.; Frydman, L. *J. Am. Chem. Soc.* **1995**, *117*, 12779.
- (9) (a) Edén, M.; Frydman, L. *J. Chem. Phys.* **2001**, *114*, 4116. (b) Edén, M.; Frydman, L. Manuscript in preparation.
- (10) (a) Madhu, P. K.; Goldbourt, A.; Frydman, L.; Vega, S. *Chem. Phys. Lett.* **1999**, *307*, 41. (b) Madhu, P. K.; Goldbourt, A.; Frydman, L.; Vega, S. *J. Chem. Phys.* **2000**, *112*, 2377.
- (11) (a) Ding, S.; McDowell, C. A. *Mol. Phys.* **1995**, *85*, 283. (b) Baldus, M.; Rovnyak, D.; Griffin, R. G. *J. Chem. Phys.* **1996**, *104*, 5902. (c) Nijman, M.; Ernst, M.; Kentgens, A. P. M.; Meier, B. H. *Mol. Phys.* **2000**, *98*, 161. (d) Joo, C.; Werner-Zwaniger, U.; Zwaniger, J. W. *Solid State NMR* **2000**, *16*, 77. (e) Dowell, N. G.; Ashbrook, S. E.; McManus, J.; Wimperis, S. *J. Am. Chem. Soc.* **2001**, *123*, 8135.

JA020534V